NACA

RESEARCH MEMORANDUM

A METHOD FOR DESIGNING LOW-DRAG NOSE-INLET—BODY COMBINATIONS FOR OPERATION AT MODERATE SUPERSONIC SPEEDS

By Robert R. Howell

Langley Aeronautical Laboratory
Langley Field, Va.

NATIONAL ADVISORY COMMITTEE FOR AERONAUTICS

WASHINGTON

November 24, 1954

NATIONAL ADVISORY COMMITTEE FOR AERONAUTICS

RESEARCH MEMORANDUM

A METHOD FOR DESIGNING LOW-DRAG NOSE-INLET—BODY COMBINATIONS FOR OPERATION AT MODERATE SUPERSONIC SPEEDS

By Robert R. Howell

SUMMARY

An experimental investigation in the Mach number range from 0.8 to 1.4 and a related analytical study have been made of the drag characteristics of axially symmetric nose-inlet—body combinations and their equivalent bodies according to the transonic area rule. It was found that pressure-drag equivalence can be obtained between an axially symmetric nose-inlet—body combination and a body of revolution having a cross-sectional-area development equal to that of the inlet body minus the cross-sectional area of the entering free-stream tube for inlet mass-flow ratios at least as low as 0.7. It was also demonstrated that the equivalent-body concept is an effective means of obtaining low-drag nose-inlet—body combinations of practical proportions for use at moderate supersonic speeds.

INTRODUCTION

Since the conception of the transonic area rule (ref. 1) much work has been done in efforts to establish the scope and limitations of its applicability. With regard to its applicability to air inlet configurations, the drag characteristics of some complex ducted configurations (refs. 2 and 3) have been examined in the light of the area rule and have been found to be at least qualitatively explainable on the basis of the longitudinal area development of the configurations.

Recently, quantitative agreement at Mach numbers up to 1.4 has been shown attainable between the pressure-drag variation of an axially symmetric nose-inlet—body combination and its equivalent body according to the transonic area rule (ref. 4). These results are of particular interest inasmuch as pressure-drag equivalence was obtained at Mach numbers substantially greater than 1.0 with the use of the transonic area

rule. On the basis of experimental results available on unducted configurations, the transonic area rule would be expected to work only at Mach numbers close to 1.0. (See ref. 1.)

The present investigation was undertaken to provide a careful check on the equivalence obtained in reference 4 and to demonstrate the effectiveness of the transonic equivalent-body concept as a basis for designing low-drag nose-inlet—body configurations. The equivalent body, for this case, was considered to be a body of revolution whose cross-sectional-area development was that of a corresponding nose-inlet—body combination less the cross-sectional area of the entering free-stream tube. In addition to an experimental investigation, a related analytical study was made to help explain the pressure-drag equivalence obtained experimentally at Mach numbers greater than 1.0.

The experimental investigation consisted of drag measurements on an arbitrary nose-inlet—body combination operating at inlet mass-flow ratios of 1.0 and 0.7 and its equivalent bodies according to the transonic area rule. The tests were conducted in the Langley transonic blowdown tunnel at a Reynolds number of about 12×10^6 based on model length and at 0° angle of attack. The Mach number range for the tests was from 0.8 to 1.41.

SYMBOLS

A	cross-sectional area
C_{D_T}	total-measured-drag coefficient, D_T/q_oF
C_{D_b}	base-drag coefficient, $\frac{D_b}{q_oF} = -\frac{(p_b - p_o)A_b}{q_oF}$
$C_{D_{in}}$	internal-drag coefficient (includes base drag), D_{in}/q_oF
$C_{D_{ext}}$	external-drag coefficient, $C_{D_T} - C_{D_i}$ or $C_{D_T} - C_{D_b}$
$\Delta C_{D_{ext}}$	difference in $C_{D_{ext}}$ at any Mach number and $C_{D_{ext}}$ at $M_o = 0.82$
$\Delta p/q$	pressure coefficient
D	drag, lb

d	diameter of body
F	maximum frontal area of $m_i/m_o = 1.0$ equivalent body
H_l/H_o	ratio of local total pressure to free-stream stagnation pressure
L	length of body or forebody
M_o	free-stream Mach number
m_i/m_o	inlet mass-flow ratio, $\frac{\rho_i V_i A_i}{\rho_o V_o A_i}$
p	static pressure
r	radius
q	dynamic pressure, $\rho V^2/2$
ρ	density
V	velocity
x	axial distance from nose leading edge

Subscripts:

o	free stream
i	inlet
b	base
C	closed body
D	ducted body
max	maximum
T	total

ANALYTICAL CONSIDERATIONS

The theory of reference 5 has been used to calculate for a Mach number of 1.41 the shapes of minimum-drag axially symmetric forebodies. The solid curves of figure 1 represent the shapes so obtained for a minimum-drag closed forebody or projectile tip of fineness ratio 6.0 and for two nose-inlet—forebody configurations having inlet to maximum diameter ratios of about 0.4 and 0.6 which bracket the range of practical interest. The minimum-drag inlet shapes are for an inlet mass-flow ratio of 1.0.

From the transonic equivalent body concept for air inlets, two other nose-inlet—forebody shapes having the same ratios of inlet to maximum diameter were derived from the longitudinal area distribution of the minimum-drag projectile tip of figure 1. The longitudinal distribution of cross-sectional area less the cross-sectional area of the entering free-stream tube of these inlet bodies is the same as the longitudinal area distribution of the closed forebody. The closed forebody or projectile tip is referred to as the equivalent body. These nose-inlet—forebody shapes are presented in figure 1 as the dashed lines. As can be seen, the difference in shapes of the forebodies obtained by the two design procedures is very small. The maximum difference at full scale would be of the order of 0.25 inch. Rough calculations indicate that, if an equivalent forebody fineness ratio of at least 3.5 is maintained, the two design procedures should, for all practical purposes, give the same shape regardless of the ratio of inlet to maximum diameter of the inlet body. It is, therefore, indicated that an axially symmetric nose-inlet—body combination having a longitudinal area distribution the same as that of a minimum-drag equivalent body should also be a minimum-drag configuration. This does not imply, however, that the value of pressure drag for all ducted configurations derived from a given area distribution will be the same as that of the equivalent body. A comparison of the pressure drag of nose-inlet—forebody combinations obtained with the equivalent-body concept with the pressure drag of their nonducted equivalent bodies can be inferred from the theory of reference 5 inasmuch as the body shapes obtained with the theory are so nearly the same as the shapes obtained from equivalent area distributions as indicated in figure 1.

The calculated pressure drag of nose-inlet—forebody combinations of varying ratios of inlet to maximum diameter are presented in figure 2 in terms of the drag of the equivalent body of figure 1 from which they were derived. It is obvious that, for a value of $d_i/d_{max} = 0$, which corresponds to the closed projectile tip or equivalent body, the drag ratio is 1.0. For increasing values of d_i/d_{max}, the inlet diameter d_i increases and, theoretically, goes to infinity for the condition of $d_i/d_{max} = 1.0$ since the area development must be maintained. The configuration corresponding to this condition $\left(d_i/d_{max} \doteq 1.0\right)$ is

[redacted]

obviously a stove pipe having zero pressure drag. For the conditions considered (M_0 = 1.41 and 2.0; $\alpha = 0^\circ$), it is seen that the pressure drag of a ducted forebody is always somewhat less than that of its equivalent nonducted forebody. However, for practical nose-inlet—body design considerations, that is, values of d_i/d_{max} up to about 0.6 and Mach numbers up to about 1.5, close agreement in pressure drag can be expected between the axially symmetric nose-inlet—body combination and its equivalent body if equivalent bodies of relatively low pressure drag are considered.

Although the difference in pressure drag between the practical inlet body and its equivalent body is indicated to be small, it may be of interest to see why this difference does exist. Figure 3 presents a comparison of the theoretical pressure distribution over a closed parabolic body of revolution of fineness ratio 12.5 and a nose-inlet—body combination having the same longitudinal area development. The pressure-coefficient calculations were made in a manner similar to that of reference 6. The inlet body has a ratio of inlet to maximum diameter of 0.6 and, of course, is operating at an inlet mass-flow ratio of unity. The calculations were made for a Mach number of 1.41 with $\alpha = 0^\circ$.

The differences in pressure drag indicated in figure 2 result from differences in pressure distributions such as those shown in figure 3. The marked differences at the extremities of the bodies result from large differences in surface slope. The particular values of pressure coefficients presented in figure 3, which were obtained for a parabolic equivalent body of revolution and corresponding ducted body, do not necessarily correspond to the theoretical values for the forebody shapes considered in figures 1 and 2. The comparison between the ducted and closed bodies in figure 3, however, should be similar to a comparison of the forebody shapes considered in figures 1 and 2. For a body which closes to a point, such as the one used in figure 3, the differences in pressure distribution on the forebody and afterbody are approximately compensating and leave the drag of both configurations nearly the same. If only the forebody and its pressures are considered, pressure-drag results comparable to those indicated in figure 2 are obtained. Although the calculations made are for a Mach number of 1.41, it is clear that the pressure distributions for the two configurations will not be identical even at a Mach number of 1.0. As was pointed out previously, however, the actual pressure-drag difference is small even at a Mach number of 1.41 and the trend with Mach number indicates that, for all practical purposes, the difference would approach a negligible amount at a Mach number of 1.0.

Another point to be noted from figure 3 is the improvement in pressure gradient over the afterbody of the inlet configuration resulting from the reduction in surface slope. This improvement in pressure gradient may have a favorable effect on the drag of the body in a viscous

fluid, although it should be noted that the wetted area of the inlet body will be greater than that of the equivalent body.

The major points to be made from this analytical study are that it should be possible to design low-drag nose-inlet—body combinations for operation at moderate supersonic speeds from the transonic equivalent-body concept and that the inlet body should never have greater pressure drag than the equivalent body from which it was derived. For practical configurations, pressure-drag equivalence can apparently be expected for supersonic Mach numbers up to at least 1.4.

MODELS

Equivalent body, $m_i/m_o = 1.0$

The equivalent body was arbitrarily selected as Lighthill's theoretical minimum-drag body (fig. 4). The shape of the body, which had a fineness ratio of 12.5, is defined by the equation

$$\frac{r}{L} = \left(\frac{r}{L}\right)_{max}\left(\sqrt{1 - x^2} - x^2\cosh^{-1}\frac{1}{x}\right)^{1/2}$$

In order to provide sufficient inlet lip thickness to permit the construction of the corresponding nose-inlet—body combination, a hemispherical nose shape was added. The radius of the hemisphere was 0.2 of the maximum radius of the body. Reference 7 indicates that a hemispherical nose shape of such small radius should have negligible effect on the drag characteristics of bodies at moderate supersonic speeds. After removal of a portion of the afterbody to allow insertion of an internal strain-gage balance and sting, the test equivalent body fineness ratio was 10.2. The body was constructed of wood and had a plastic external finish. The external shape and dimensions are presented in figures 4 and 5 and table I.

Nose-Inlet—Body Combination

The area distribution of the inlet mass-flow-ratio-1.0 equivalent body was added to an imaginary cylinder to obtain the external shape of the inlet body; that is, the entering free-stream tube was handled in the same manner as in references 3 and 4. The ratio of inlet to maximum diameter was chosen to be 0.53 with a resultant total fineness ratio of 8.9. The external shape and ordinates are presented in figures 4

and 5 and table I. The internal open-area distribution is shown in figure 6. A sketch of the model in cross section (fig. 4) shows the details of the internal ducting arrangement. For the tests at an inlet mass-flow ratio of 0.7, an internal constriction was used to obtain the reduced flow rate. The model was constructed of stainless steel and had a highly polished external surface.

Equivalent Body, $m_i/m_o = 0.7$

The area distribution for the $m_i/m_o = 0.7$ equivalent body was obtained by removing from the cross-sectional area of the nose-inlet—body combination the cross-sectional area of the entering free-stream tube at the $m_i/m_o = 0.7$ condition. This removal of area results in an equivalent body having a blunt nose as shown in figure 5. The model was constructed of wood with a plastic external finish. The external body ordinates are presented in table I.

Reference 3 suggested the possibility that pressure-drag equivalence between an inlet body and its equivalent body for the reduced-inlet mass-flow-ratio condition could be attained only if the growth of the entering free-stream tube ahead of the inlet was considered part of the area development of the inlet body. Some tests were made to investigate this possibility. The growth in cross-sectional area of the entering free-stream tube was estimated by using the theory of reference 8 to locate the inlet bow shock and by making an arbitrary fairing between the shock and the inlet lip. The longitudinal growth of cross-sectional area of the entering free-stream tube obtained was reproduced as spikes which were placed ahead of the blunt-faced equivalent body for some of the tests. Spikes designed for $M_o = 1.25$ and $M_o = 1.40$ (fig. 4) were tested. An arbitrarily rounded nose ahead of the blunt-faced equivalent body was also tested.

APPARATUS AND TESTS

The models were sting-mounted in the wind tunnel at 0° angle of attack (figs. 4 and 7). The angle of attack of the model was established by means of a sensitive inclinometer and was unchanged for the tests.

Total-pressure measurements were made at the exit of the inlet body by use of a 13 total-pressure-tube rake which was clamped to the sting and was free of the model (fig. 4). The distribution of total-pressure tubes is shown in figure 8 and typical total-pressure measurements are presented in figure 9. The static pressure at the base of the models was measured by inserting an open-end tube through the center of the

sting into an open section of the balance. For the equivalent bodies, the pressure measured was the average pressure in the annular opening around the sting in the plane of the model base. For the inlet body, the pressure measured was the average in the annular opening between the balance shield and the sting in the plane of the model base. (See enlarged sketch, fig. 4.) These static pressures were used to adjust the base pressure drag to that corresponding to free-stream static pressure, and in the case of the inlet model, were used in conjunction with the measured total pressures to obtain point values of momentum deficit and mass-flow ratio. These point values were in turn numerically integrated over the annular area of the exit to obtain inlet mass-flow ratio and internal drag.

For most of the tests with artificially fixed boundary-layer transition, a 1/4-inch-wide band of 0.003-inch- to 0.005-inch-diameter carborundum particles was placed around the bodies 1/4 inch behind the leading edge. For the mass-flow-ratio-1.0 equivalent body, a 1/2-inch-wide band was used.

Most of the tests were made in the Langley transonic blowdown tunnel. This tunnel has an octagonal slotted test section, 26-inches between flats. The tests covered a range of Mach number from 0.81 to 1.41 and a corresponding range of Reynolds number from 11.6×10^6 to 13.7×10^6 based on model length. Because of the small ratio of model to tunnel size used, tunnel-wall interference effects are thought to be negligible at subsonic speeds (ref. 9). In the low supersonic Mach number range (between $M_o = 1.03$ and $M_o \cong 1.16$), wall-reflected bow-shock effects prevent the data from being comparable to free-air results. The effects of small static-pressure gradients along the tunnel center line in the region of the model at Mach numbers from 1.16 to 1.35 were eliminated by applying buoyancy corrections to the drag data in this Mach number range. To provide an experimental check on the accuracy of these corrections and also to provide a guide in fairing the drag curves through the bow-shock-reflection interference range, the $m_i/m_o = 1.0$ equivalent body was tested in the Langley 8-foot transonic pressure tunnel through a range of Mach number from 0.90 to 1.21 at a Reynolds number of about 2.0×10^6 based on model length. The results of this test should be comparable to free-air results except in the Mach number range between 1.00 and 1.02 where the bow-shock reflection interfered with the model. Model conditions for the two tests in the different facilities were the same except for a difference in sting configurations which resulted in a slightly different base-pressure drag.

The estimated maximum possible error in C_{D_T}, $C_{D_{ext}}$, and M_o based on the accuracy of individual measurements and the repeatability of data is ± 0.002, ± 0.005, and ± 0.01, respectively.

[redacted]

RESULTS AND DISCUSSION

The measured drag components and inlet mass-flow ratios for the configurations tested are presented as a function of Mach number in figure 10. All drag coefficients presented are based on the frontal area of the $m_1/m_0 = 1.0$ equivalent body. Consequently, relative values determined from comparisons of drag coefficients correspond to relative values of drag force.

Approximate limits to the bow-shock-reflection interference range are evidenced by the depression in the drag curves between Mach numbers of about 1.03 and 1.16. Some data were obtained in the interference Mach number range to help define the interference region. These data are faired with dashed lines in figure 10, whereas the estimated interference-free external-drag curves in this region are faired with solid lines.

High Inlet Mass-Flow Ratio

Equivalent body, $m_1/m_0 = 1.0$.- The results of the tests in the Langley 8-foot transonic pressure tunnel were used as a guide to fair through the reflection interference range for the $m_1/m_0 = 1.0$ equivalent body (fig. 10(a)). Comparison of the data obtained from the two test facilities indicates that the buoyancy correction applied to the data of the Langley transonic blowdown tunnel is essentially correct, and that the presented data should be comparable to free-air results outside the bow-shock-reflection interference range.

Addition of a roughness strip at the model nose had negligible effect on the external drag throughout the speed range. Schlieren observations indicated that at supersonic speeds this effect was due to an overexpansion at the nose of the model followed by a compression shock which apparently fixed transition at the nose for these speeds. An expansion around the hemispherical nose followed by an adverse pressure gradient which fixed transition probably also occurred at subsonic speeds although there are no pressure-distribution data available to verify this possibility.

Ducted body, $m_1/m_0 \approx 1.0$.- The maximum inlet mass-flow ratio achieved (fig. 10(b)) was slightly less than the desired value of 1.0. This probably resulted from a constricting effect due to boundary-layer growth in the short length of constant-area duct which followed the inlet. The length of constant-area duct was required to provide sufficient metal thickness in the vicinity of the inlet lip to meet the model structural requirements.

[redacted]

The addition of a transition strip at the model nose had no effect on the external drag at subsonic speeds, which is probably due to flow spillage at the lower inlet mass-flow ratios around the relatively sharp lip which prevented attainment of laminar flow. However, at supersonic Mach numbers (where the inlet mass-flow ratio was close to 1.0), some laminar flow was apparently obtained.

Also shown in figure 10(b) are the supersonic drag coefficients for inlet body III (m_i/m_o = 1.0) of reference 10. The estimated fin drag has been removed and the drag coefficients have been converted to a basis corresponding to those of the present inlet body. The supersonic drag level of the present inlet body was about 30 percent lower than that of the reference inlet body which was the best nose-inlet—body combination previously tested in this Mach number range. This large reduction in drag should not be associated entirely with the present design procedure since a major portion of the reduction could be accounted for by the difference in fineness ratio between the two test models. The comparison was made primarily to show the possible gains in performance through more optimum inlet-body designs.

Comparison of drag characteristics of inlet body and its equivalent body, m_i/m_o = 1.0.- The pressure- and external-drag characteristics of the inlet body at a mass-flow ratio of 1.0 are compared with the characteristics of its equivalent body in figure 11. The drag coefficients at a mass-flow ratio of 1.0 were obtained by means of a linear extrapolation of the data presented in figure 10. The data for the transition-fixed condition were used for the extrapolation in order to avoid the effects of any possible shifts in transition point with change in mass-flow ratio. As can be seen in figure 11, the variation of pressure drag with Mach number for the two configurations was essentially identical. In addition, the absolute values of the external drag were also very nearly the same. The small difference in drag that did exist between the two configurations at subsonic speeds was about one-half the amount expected on the basis of the difference in wetted area. This result, also obtained in reference 4, is believed to be due to an improvement in pressure gradient over the afterbody of the inlet configuration as previously noted in the section "Analytical Considerations."

Reduced Inlet Mass-Flow Ratio

Comparison of drag characteristics of inlet body and its equivalent body, m_i/m_o = 0.7.- The pressure- and external-drag characteristics of the inlet body at a mass-flow ratio of 0.7 are compared with the characteristics of its equivalent body in figure 12. As in the mass-flow-ratio-1 case, pressure-drag variations with Mach number for the two configurations were in good agreement. A maximum difference in pressure

drag occurred at a Mach number of 1.4 and amounted to 0.02 in drag coefficient. This small difference is within the experimental accuracy of most test facilities. The absolute value of the external drag for the two configurations was again nearly the same.

Effect of spikes.- It was pointed out previously that spikes simulating the growth in cross-sectional area of the free-stream tube entering the inlet at an inlet mass-flow ratio of 0.7 were tested in conjunction with the $m_i/m_o = 0.7$ equivalent body to determine if this area growth ahead of the inlet should be considered a part of the geometric area development of the inlet body at reduced inlet flow rates. As can be seen in figures 10(c) and 12, the major effect of the spikes was to reduce the external drag of the equivalent body by about a constant value throughout the test Mach number range. The variation of pressure drag with Mach number, therefore, was the same with or without spikes.

Tests of the $M_o = 1.4$ design spike, the $M_o = 1.25$ design spike, and of the arbitrarily rounded nose gave the same reductions in external drag. The indications are, therefore, that the external drag reduction was due to an improvement in surface slope at the blunt face of the equivalent body but did not depend on the detailed contour used. Apparently, the reduction in surface slope and consequent reduction in turning of the flow at the nose of the model reduced the adverse effects of local boundary-layer separation that probably existed at the nose of the blunt-faced equivalent body.

Schlieren photographs of the flow at the nose of the inlet body at a mass-flow ratio of 0.7 and the $m_i/m_o = 0.7$ equivalent body for Mach numbers of 1.1 and 1.3 (fig. 13) show that the presence of the spikes or round nose did not alter to any significant degree the supersonic flow field in the vicinity of the nose, which is consistent with the agreement in pressure drag for the different nose shapes tested (fig. 12). Also, note the agreement of shock location and similarity of basic flow phenomena between the inlet body and its blunt-faced equivalent body, especially at $M_o = 1.3$.

Performance

At supersonic speeds, where the total-pressure recovery at the inlet station is primarily dependent on Mach number, relative performance of normal-shock open-nose-inlet—body combinations can be judged on the basis of external-drag characteristics. The external drag at a given Mach number can be determined from the drag at $m_i/m_o = 1.0$ (minimum drag) and the variation of drag with mass-flow ratio. A comparison of the rate of change of external drag with inlet mass-flow ratio of the present inlet body with the two best bodies of reference 10 is made in

figure 14 for the Mach number range from 1.0 to 1.4. The slopes for the present configuration were determined by using the data for transition fixed to eliminate any effect of possible shifts of transition point. Also shown in figure 14 is the theoretical additive drag of reference 11, which is indicative of the maximum possible drag due to spillage.

It is seen that, in addition to having lower drag at $m_i/m_o = 1.0$ (fig. 10(b)), the present configuration also has lower values of the variation of external-drag coefficient with inlet mass-flow ratio throughout the Mach number range investigated, indicating a relatively large improvement in overall performance.

CONCLUSIONS

An experimental investigation in the Mach number range between 0.8 and 1.4 with 0° angle of attack and a related analytical study have been made of the drag characteristics of axially symmetric nose-inlet—body combinations and their equivalent bodies according to the transonic equivalent-body concept. The following conclusions are indicated:

1. Pressure-drag equivalence can be obtained between an axially symmetric nose-inlet—body combination and a body of revolution having a cross-sectional-area development equal to that of the inlet body minus the cross-sectional area of the entering free-stream tube for inlet mass-flow ratios at least as low as 0.7 and Mach numbers up to at least 1.4.

2. The use of the equivalent-body concept has been demonstrated as an effective means of obtaining low-drag nose-inlet—body combinations of practical proportions for operation at moderate supersonic speeds.

Langley Aeronautical Laboratory,
National Advisory Committee for Aeronautics,
Langley Field, Va., August 19, 1954.

[redacted]

REFERENCES

1. Whitcomb, Richard T.: A Study of the Zero-Lift Drag-Rise Characteristics of Wing-Body Combinations Near the Speed of Sound. NACA RM L52H08, 1952.

2. Sears, Richard I.: Some Considerations Concerning Inlets and Ducted Bodies at Mach Numbers From 0.8 to 2.0. NACA RM L53I25b, 1953.

3. Keith, Arvid L., Jr.: Transonic Wind-Tunnel Investigation of the Effects of Body Indentation on the Aerodynamic Characteristics of a Semielliptical Sweptback Wing-Root Inlet Configuration. NACA RM L54A29, 1954.

4. Walters, Richard E.: Application of Transonic Area Rule to a Sharp-Lipped Ducted Nacelle. NACA RM L53J09b, 1954.

5. Parker, Hermon M.: Minimum-Drag Ducted and Pointed Bodies of Revolution Based on Linearized Supersonic Theory. NACA TN 3189, 1954.

6. Jones, Robert T., and Margolis, Kenneth: Flow Over a Slender Body of Revolution at Supersonic Velocities. NACA TN 1081, 1946.

7. Wallskog, Harvey A., and Hart, Roger G.: Investigation of the Drag of Blunt-Nosed Bodies of Revolution in Free Flight at Mach Numbers From 0.6 to 2.3. NACA RM L53D14a, 1953.

8. Moeckel, W. E.: Approximate Method for Predicting Form and Location of Detached Shock Waves Ahead of Plane or Axially Symmetric Bodies. NACA TN 1921, 1949.

9. Wright, Ray H., and Ward, Vernon G.: NACA Transonic Wind-Tunnel Test Sections. NACA RM L8J06, 1948.

10. Sears, R. I., Merlet, C. F., and Putland, L. W.: Flight Determination of Drag of Normal-Shock Nose Inlets With Various Cowling Profiles at Mach Numbers From 0.9 to 1.5. NACA RM L53I25a, 1953.

11. Sibulkin, Merwin: Theoretical and Experimental Investigation of Additive Drag. NACA RM E51B13, 1951.

[redacted]

TABLE I.- EXTERNAL DESIGN DIMENSIONS

x	Ducted body, r	Equivalent body, r; m_1/m_o = 1.0	Equivalent body, r; m_1/m_o = 0.7
0	0.3000	0	0.164
.018	.3048	.054	.1730
.036	.3085	.072	.1794
.048	.3112	.0826	.1839
.072	.3127	.0882	.1865
.090	.3132	.0900	.1874
.100	.3139	.0923	.1885
.200	.3183	.1065	.1958
.280	.3218	.1164	.2014
.580	.3376	.1548	.2257
.880	.3549	.1896	.2509
1.180	.3732	.2220	.2762
1.480	.3918	.2520	.3008
1.780	.4101	.2796	.3243
2.080	.4285	.3060	.3473
2.380	.4460	.3300	.3686
2.680	.4622	.3516	.3881
2.980	.4779	.3720	.4067
3.280	.4930	.3912	.4243
3.580	.5074	.4092	.4410
3.880	.5201	.4248	.4555
4.180	.5329	.4404	.4701
4.480	.5428	.4524	.4813
4.780	.5519	.4632	.4915
5.080	.5589	.4716	.4994
5.380	.5640	.4776	.5051
5.680	.5660	.4800	.5073
5.980	.5640	.4776	.5051
6.280	.5589	.4716	.4999
6.580	.5519	.4632	.4915
6.880	.5428	.4524	.4813
7.180	.5329	.4404	.4701
7.480	.5201	.4248	.4555
7.780	.5074	.4092	.4410
8.080	.4930	.3912	.4243
8.380	.4779	.3720	.4067
8.680	.4622	.3516	.3881
8.980	.4460	.3300	.3686
9.280	.4285	.3060	.3473
9.580	.4101	.2796	.3243
9.800	.407	.255	.3033

[redacted]

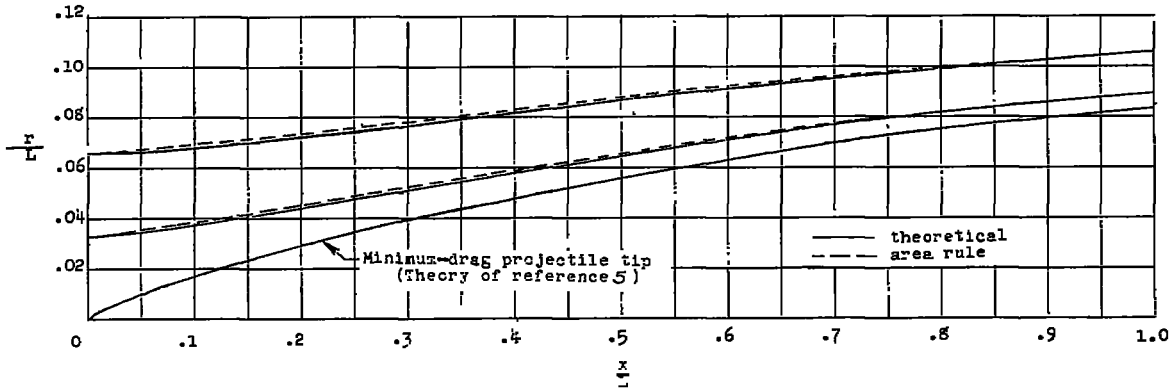

Figure 1.- Comparison of forebody shapes of ducted bodies obtained by theory of reference 5 and those obtained by wrapping the area distribution of the projectile tip of reference 5 about cylinders equal to the inlet area in cross section.

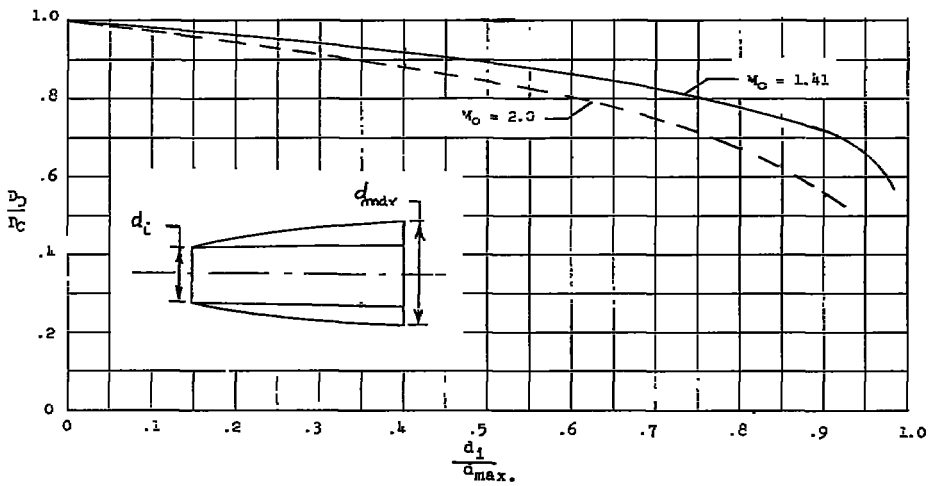

Figure 2.- Variation of ratio of ducted forebody drag to closed equivalent forebody drag with inlet to maximum diameter ratio for $M_o = 1.41$ and $M_o = 2.0$. $\alpha = 0^o$.

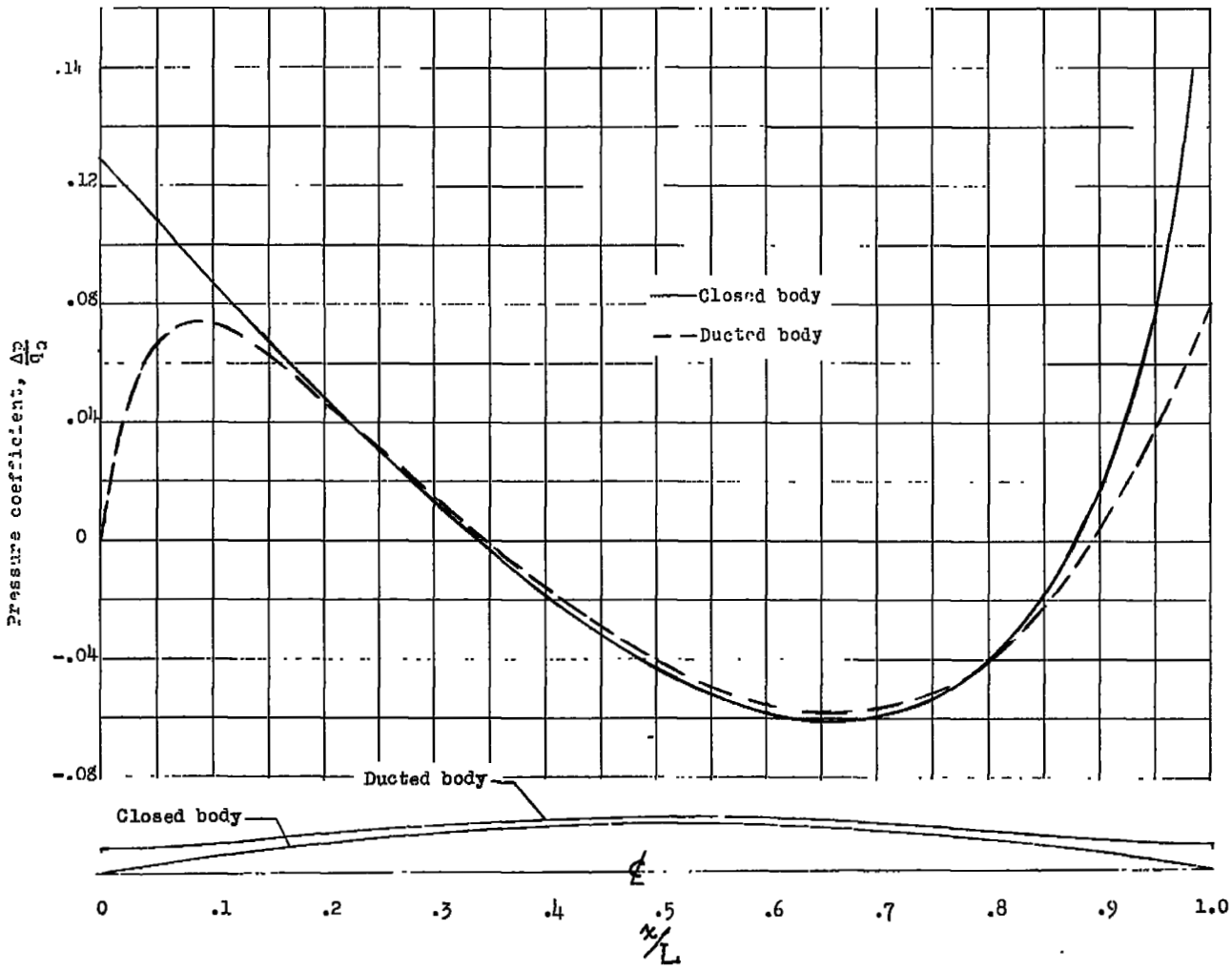

Figure 3.- Comparison of pressure distribution over parabolic body of revolution and nose-inlet—body combination $\left(d_i/d_{max} = 0.6;\ m_i/m_o = 1.0\right)$ having the same longitudinal area development. $M = 1.41$; $\alpha = 0^o$.

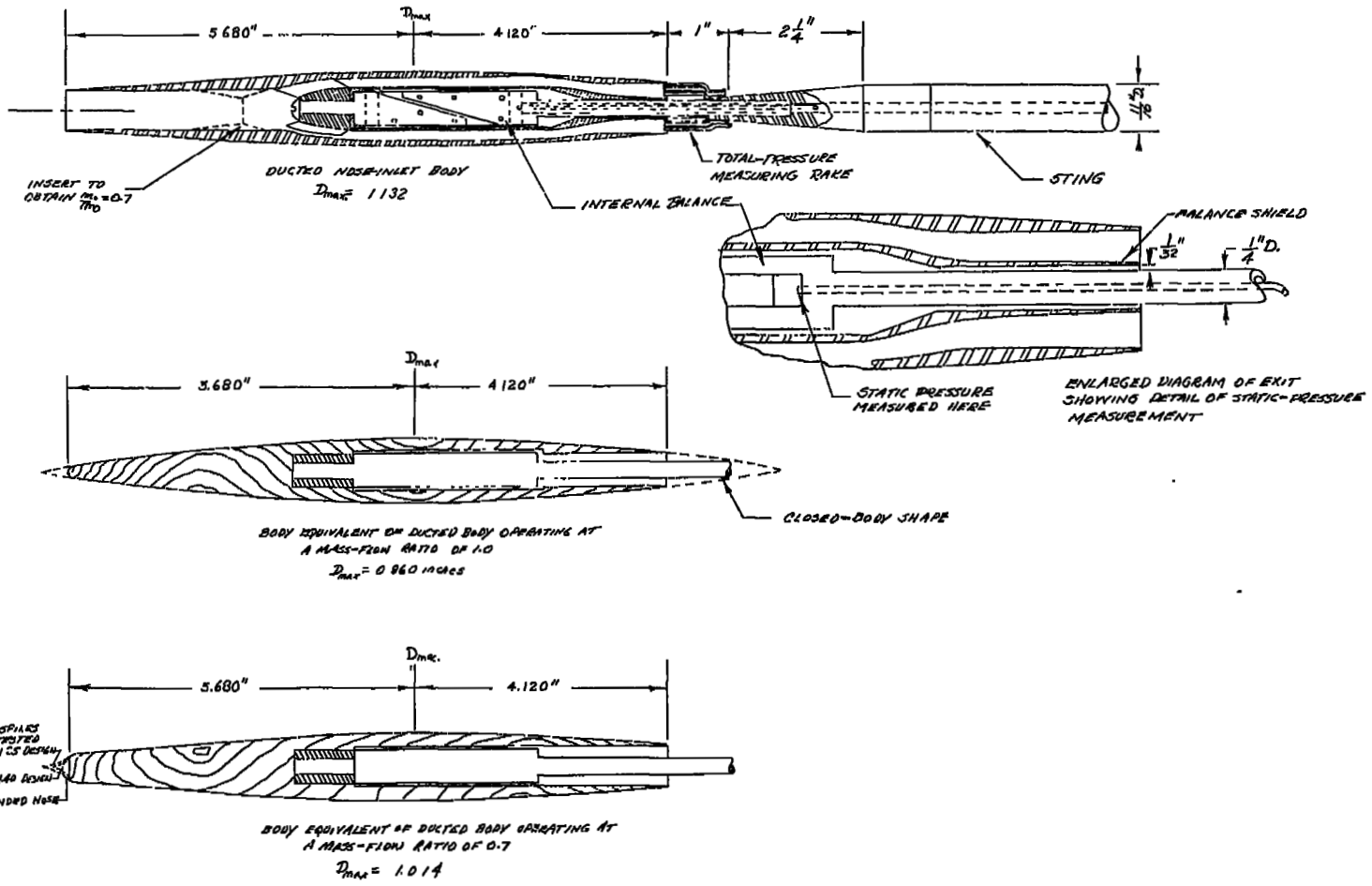

Figure 4.- Diagrammatic sketch of the three configurations tested.

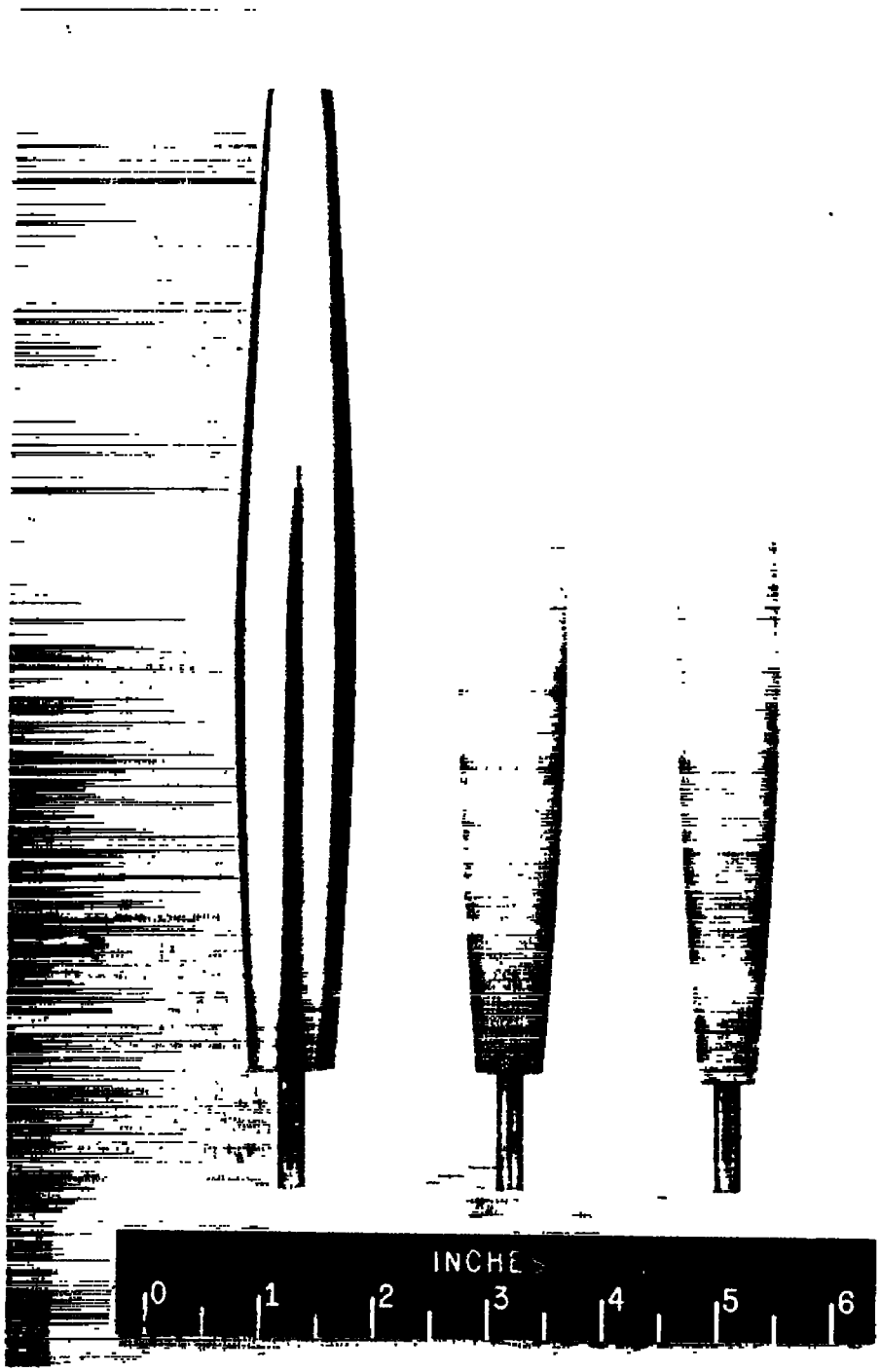

L-84141

Figure 5.- Photograph of the three bodies tested.

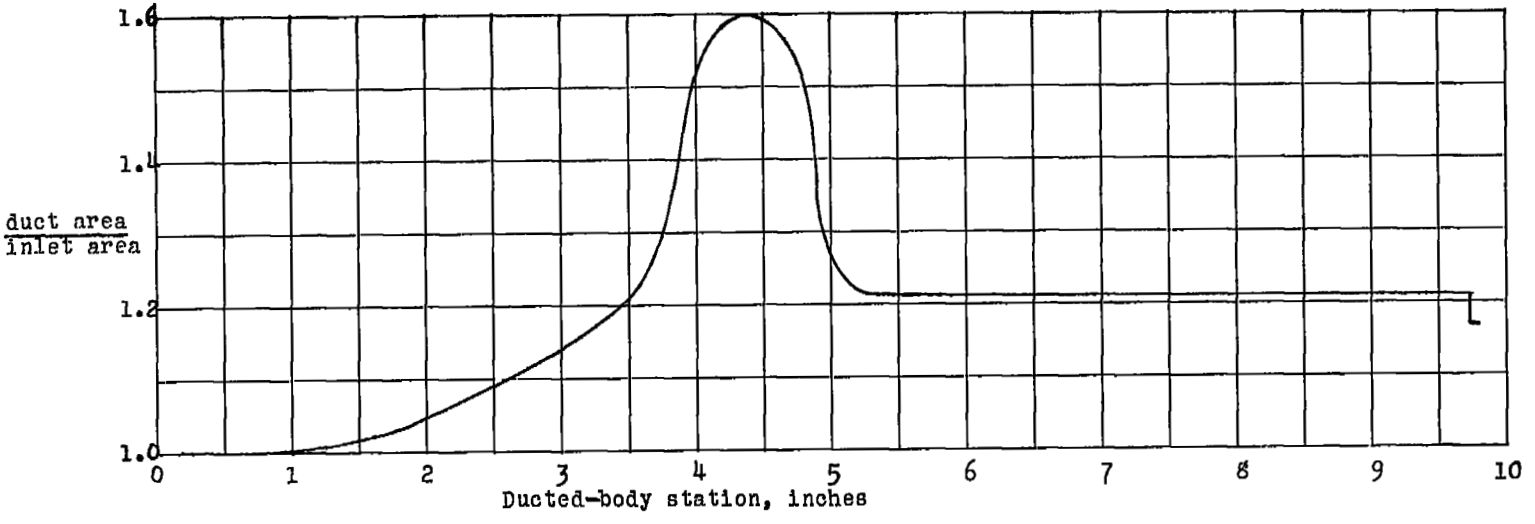

Figure 6.- Distribution of internal-duct cross-sectional area.

L-83178

Figure 7.- Photographs showing $m_i/m_o = 1.0$ equivalent body mounted in tunnel.

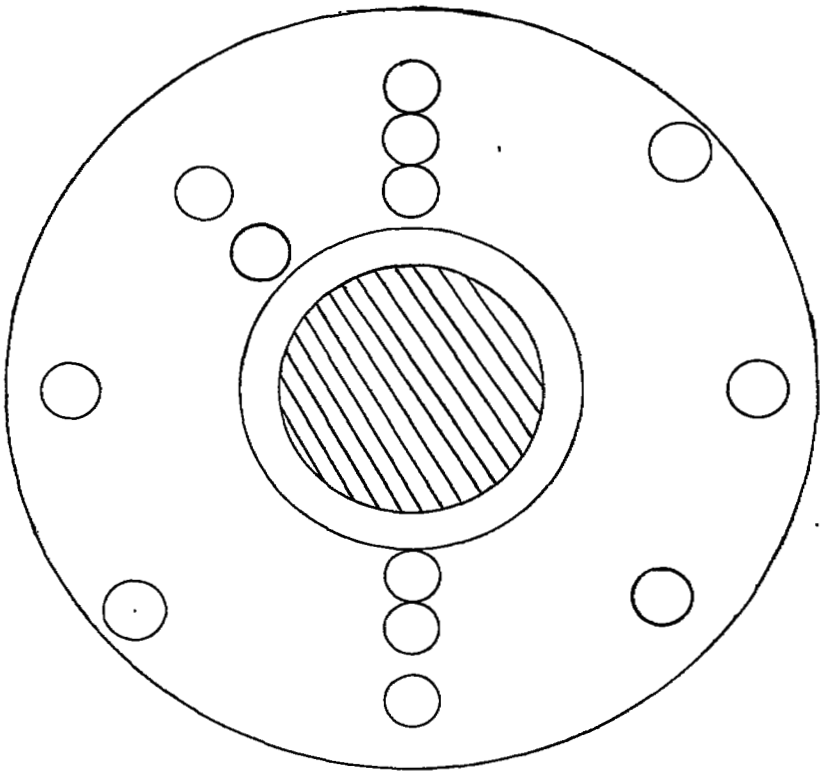

Figure 8.- Distribution of total-pressure tubes in exit measuring rake.

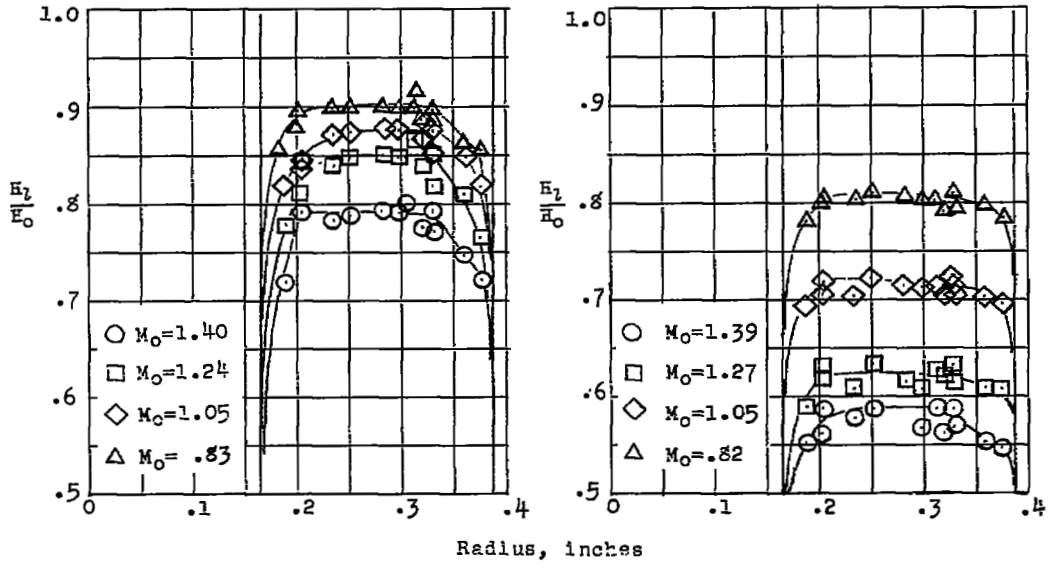

Figure 9.- Typical total-pressure measurements made at exit station for the two inlet mass-flow ratios investigated.

[redacted]

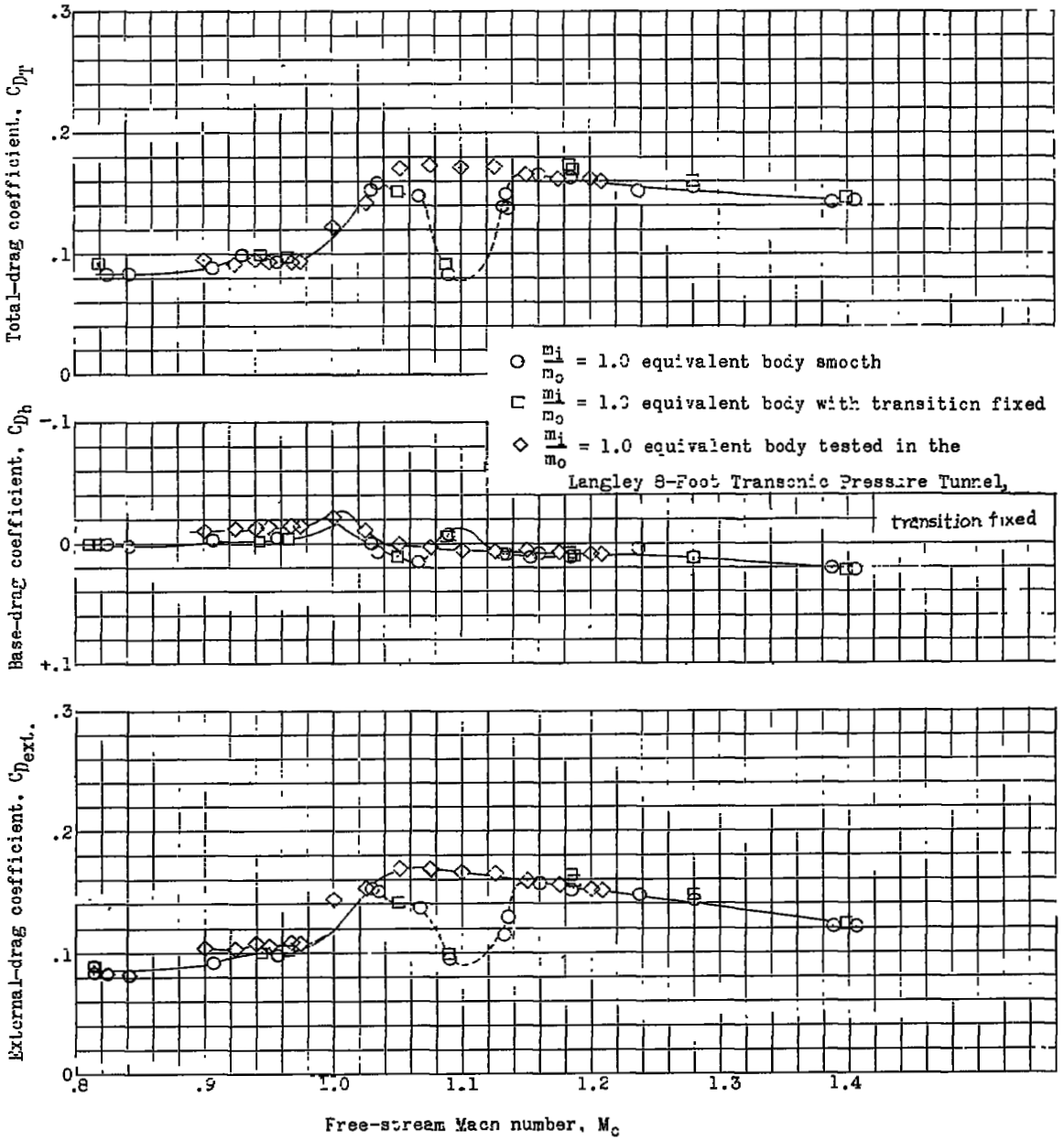

(a) Basic body $\left(m_1/m_o = 1.0 \text{ equivalent body}\right)$.

Figure 10.- Variation of measured drag components and mass-flow ratio of configuration tested with Mach number.

[redacted]

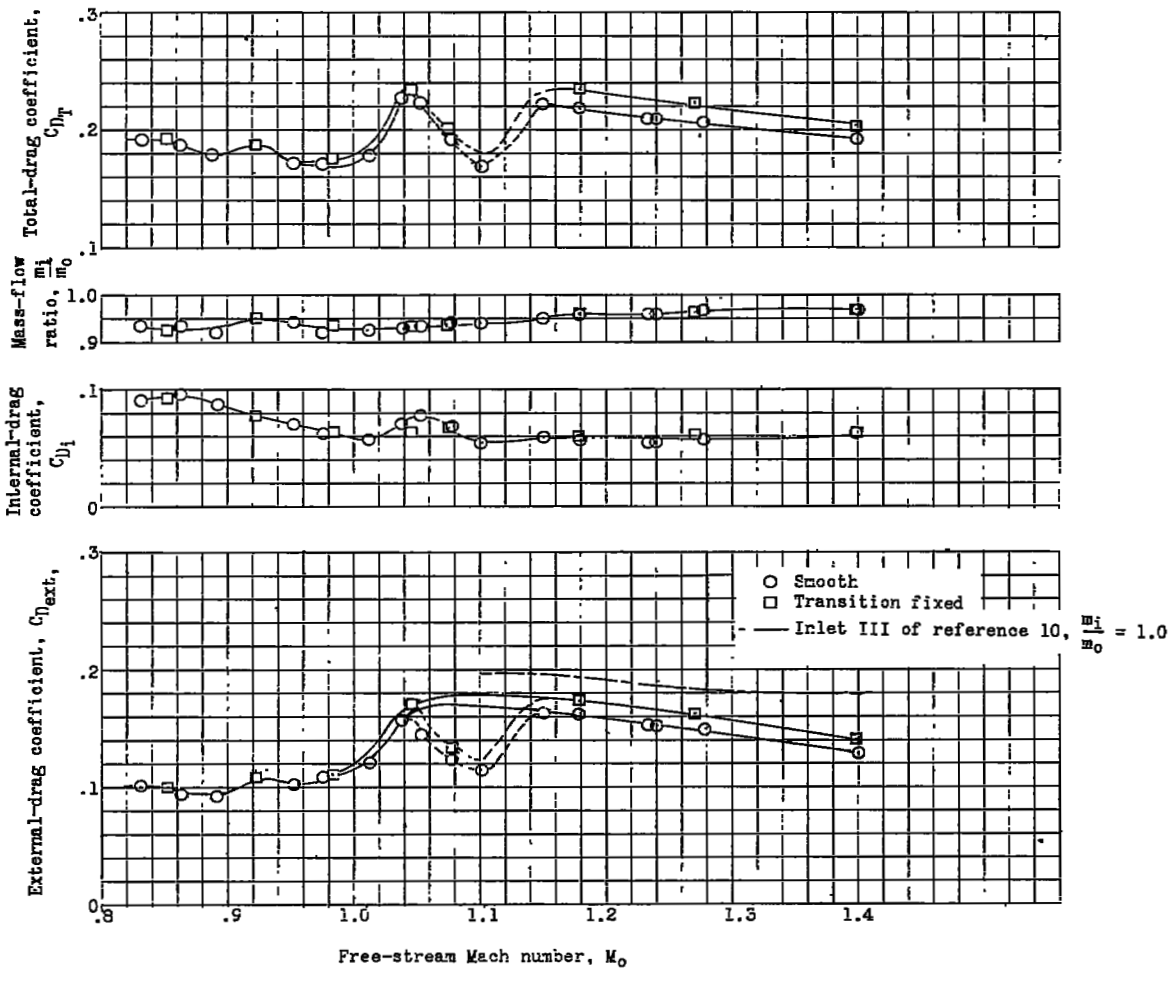

(b) Ducted body (high flow rate).

Figure 10.- Continued.

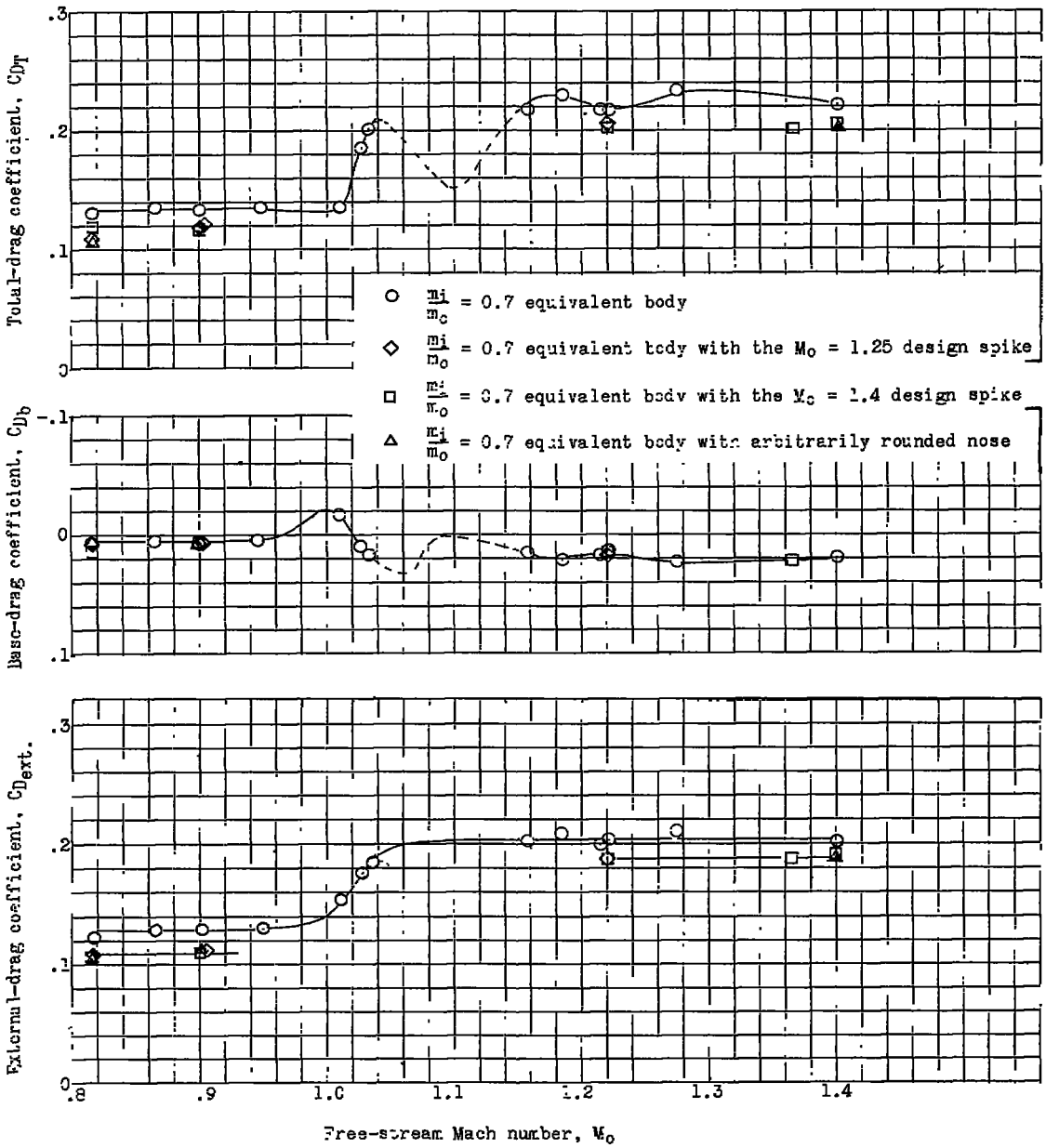

(c) $m_i/m_o = 0.7$ equivalent body.

Figure 10.- Continued.

[redacted]

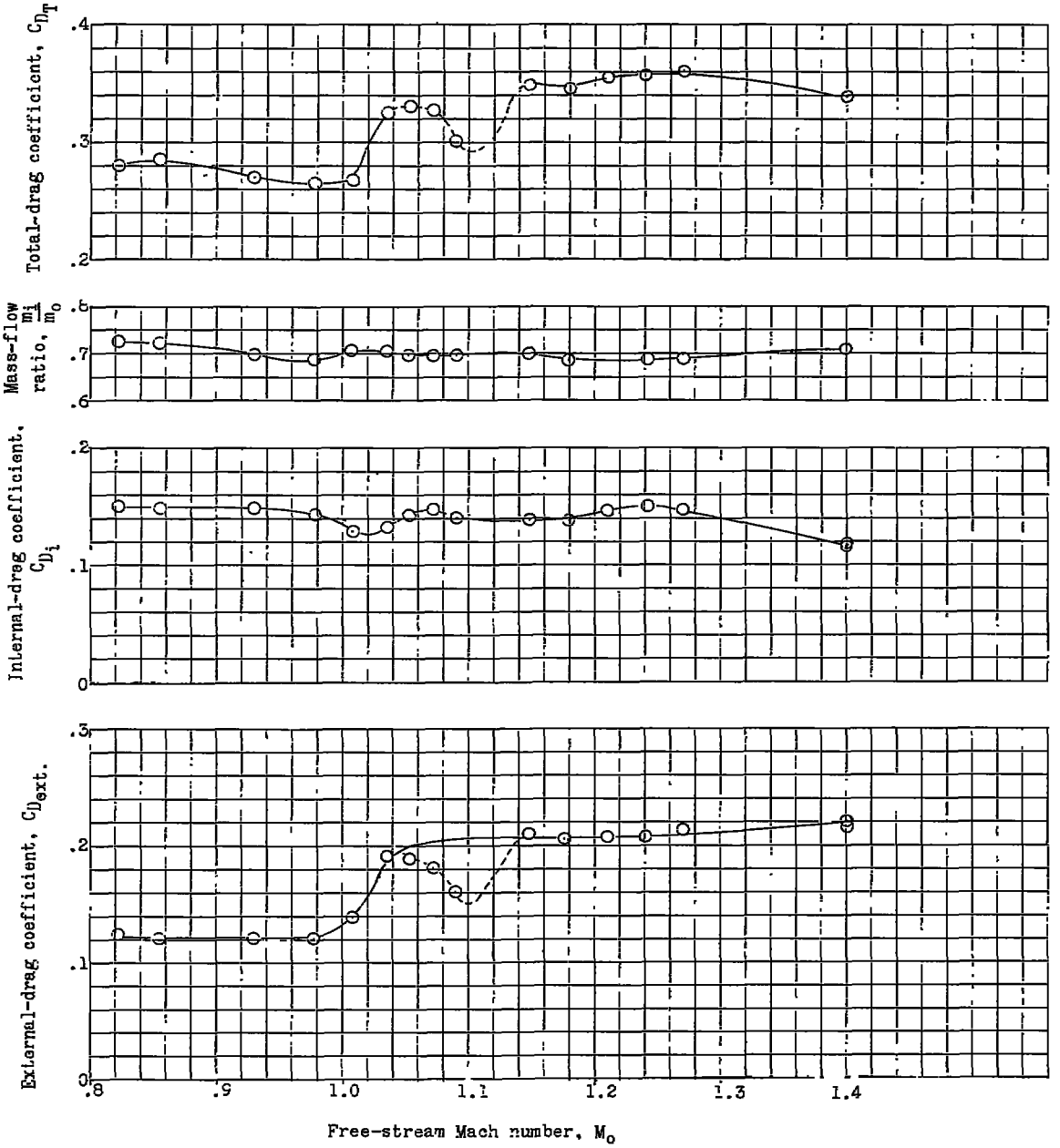

(d) Ducted body $\left(m_i/m_o \cong 0.7\right)$.

Figure 10.- Concluded.

[redacted]

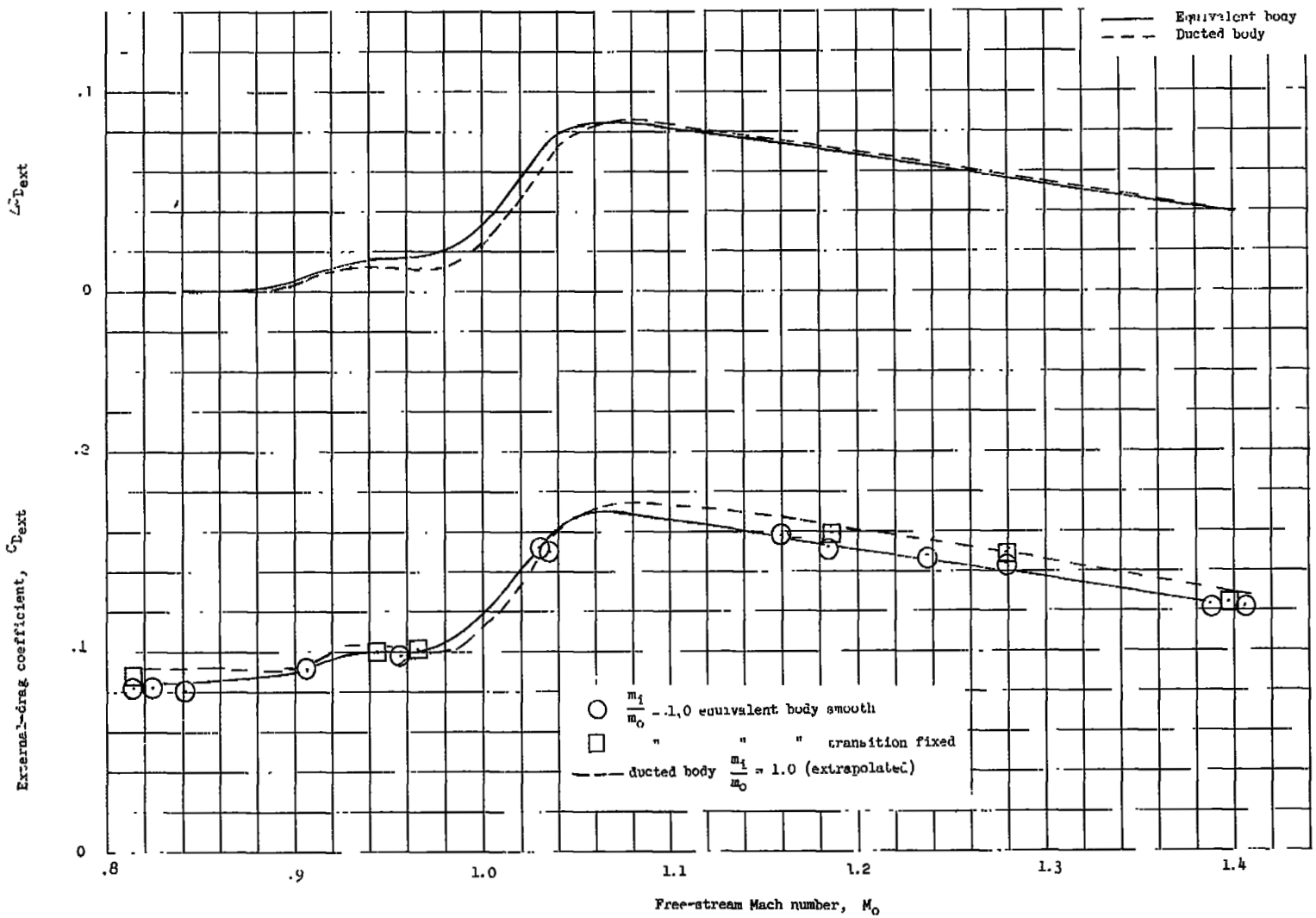

Figure 11.- Comparison of external drags of ducted and equivalent bodies. $m_i/m_o = 1.0$.

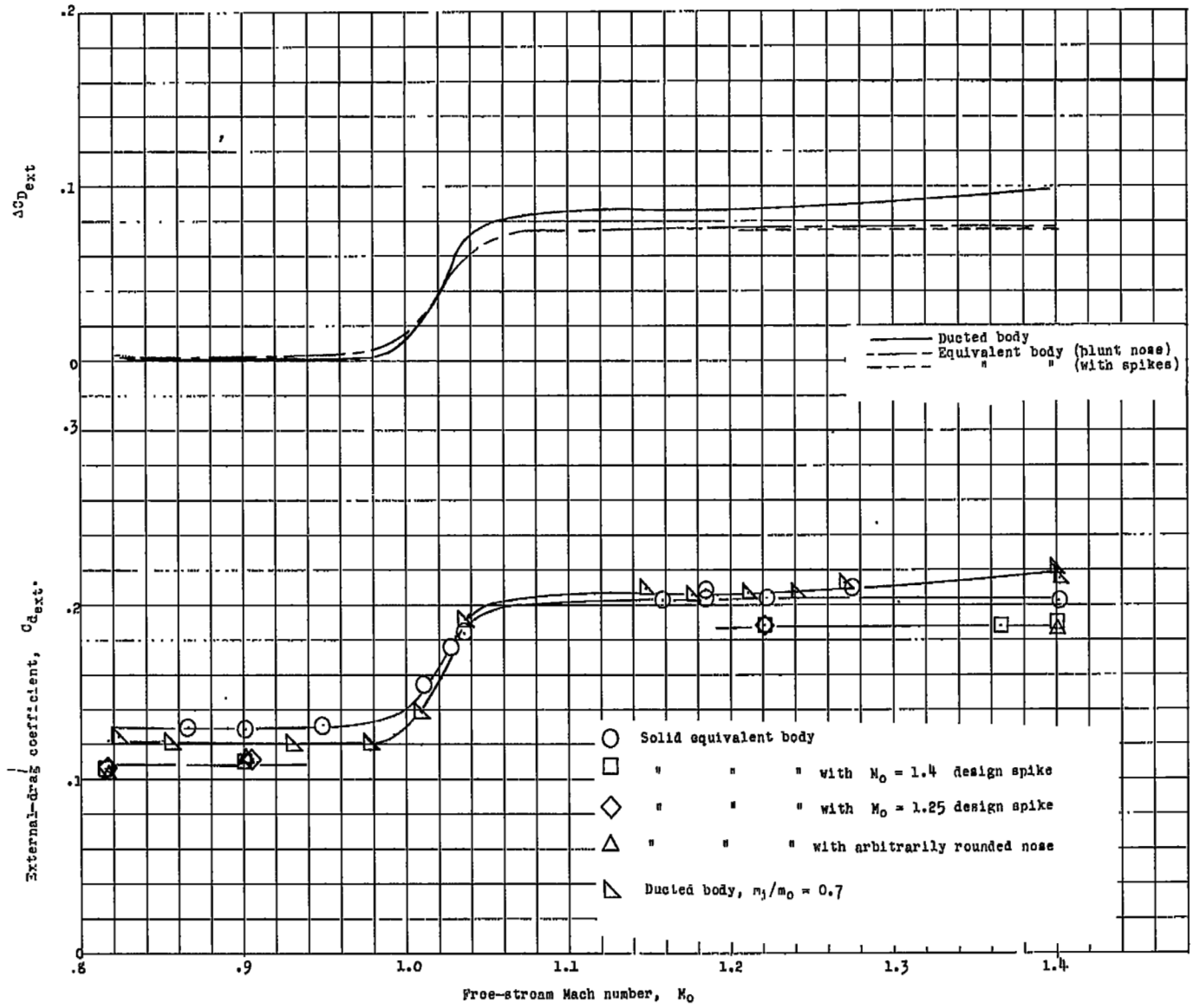

Figure 12.- Comparison of external drags of ducted and equivalent bodies. $m_j/m_o = 0.7$.

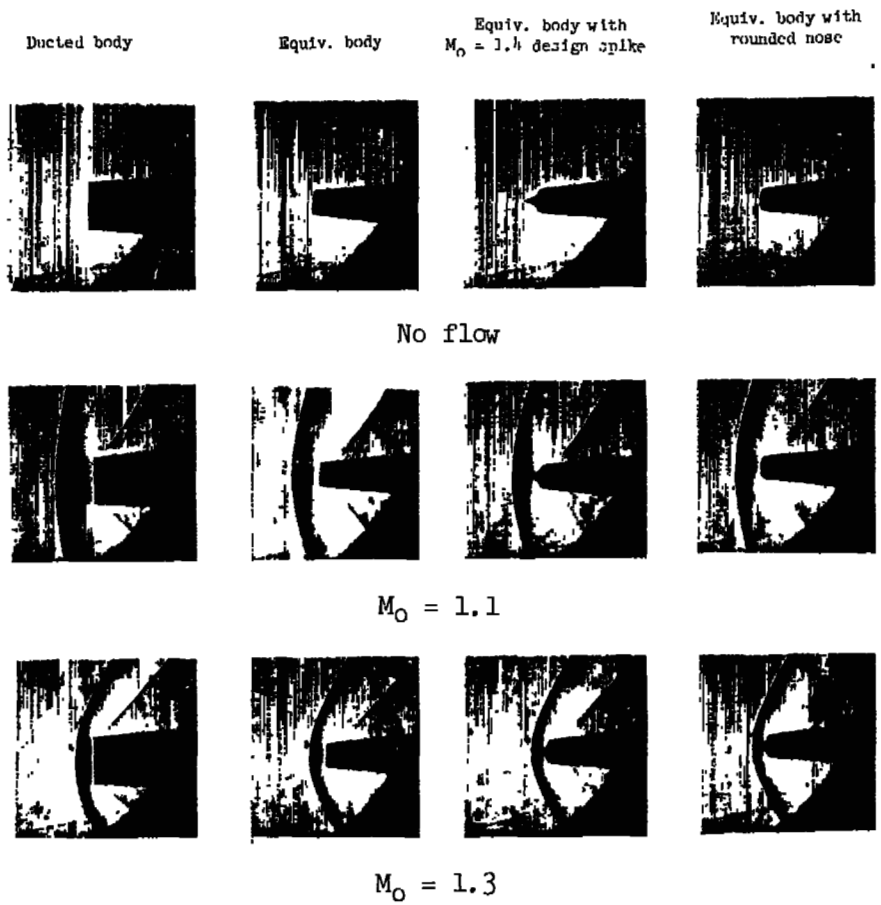

L-85651

Figure 13.- Comparison of schlieren photographs of flow at nose of ducted body $\left(m_i/m_o = 0.7\right)$ and various equivalent bodies at Mach numbers of 1.1 and 1.3.

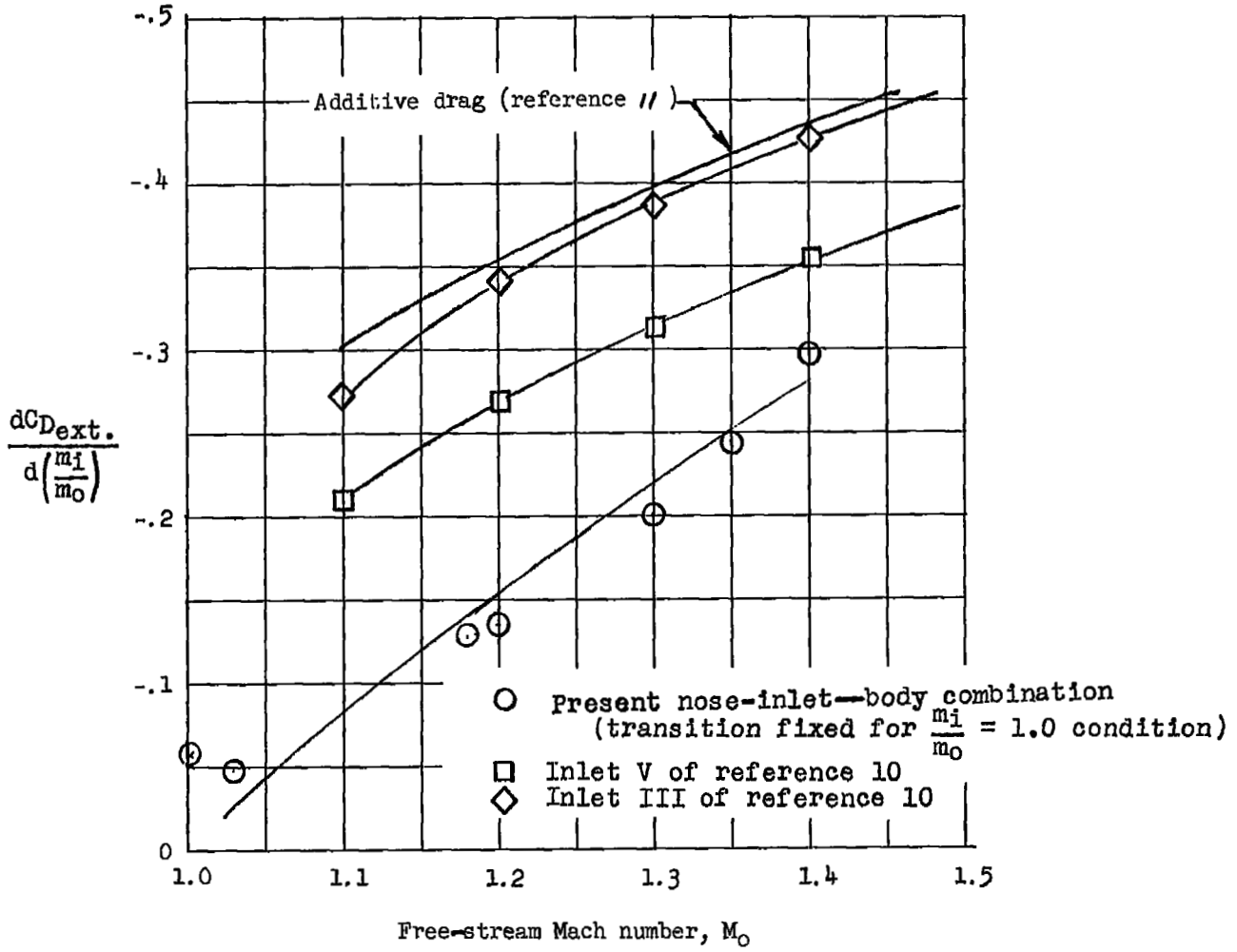

Figure 14.- Comparison of rate of change of external-drag coefficient with inlet mass-flow ratio of present nose-inlet—body combination and nose-inlet—body combinations of reference 10 for Mach number range between 1.0 and 1.4.